H4.SMR/210 - 32

SPRING COLLEGE ON PLASMA PHYSICS

(25 May - 19 June 1987)

PRESHOCK REGION ACCELERATION OF
IMPLANTED COMETARY H+ AND O+

T.I. GOMBOSI

University of Michigan
Ann Arbor, MI 48109
U.S.A.

PRESHOCK REGION ACCELERATION OF IMPLANTED COMETARY H+ AND O+

Tamás I. Gombosi*

Space Physics Research Laboratory
Department of Atmospheric and Oceanic Science
The University of Michigan
Ann Arbor, MI 48109

May 1987
Submitted to: Journal of Geophysical Research

* also at Central Research Institute for Physics, Budapest, Hungary.

Abstract

One of the most interesting results of the cometary flyby missions was the realization that magnetohydrodynamic turbulence generated by the pickup process of freshly ionized cometary particles results in fast pitch-angle scattering of the newly implanted ions. This process rapidly modifies the newly implanted ion pitch-angle distribution in the solar wind frame of reference from the original pickup ring to a pickup shell distribution. It also seems to be established that the implanted ions have an isotropic pitch-angle distribution in the decelerating solar wind frame of reference. This paper presents a self-consistent description of the multispecies plasma flow (composed of solar solar wind, cometary H^+ and O^+) in the unshocked upstream region. The solar wind is treated as a fluid, while the evolution of the implanted ion distributions is described by generalized transport equations. Solar wind particles are not produced (the cometary hydrogen is treated as different species) and are depleted by charge exchange. The transport equations take into account the adiabatic velocity change due to the deceleration of the flow, velocity diffusion, charge exchange loss, and the pickup of newly created ions. The model equations were numerically solved for comet Halley flyby conditions, and the results are compared with spacecraft observations. Our calculations imply that second order Fermi acceleration can explain the implanted spectra observed in the unshocked solar wind. The comparison of the measured and calculated distribution functions also indicate that field aligned transport of implanted ions potentially plays an important role in forming the energetic particle environment of active comets.

Introduction

It was recognized some twenty years ago (Biermann et al. 1967) that the expanding cometary exosphere represents an extensive, "soft" obstacle for the supersonic and superalfvenic solar wind flow. The resulting interaction pattern is very much different from the solar wind interaction with other solar system bodies with gravitationally bound dense atmospheres and/or significant intrinsic magnetic fields. Neutral atoms and molecules of cometary origin, which at large cometocentric distances ($r \leq 10^4$ km) move along ballistic trajectories with velocities ranging from ~0.5 km/s to a few tens of km/s, become ionized due to photoionization or charge exchange with a characteristic ionization lifetime of 10^5 - 10^7 seconds (cf. Gombosi et al. 1986). The ionization process introduces a new, practically stationary charged particle into a high speed magnetized flow. In their pioneering work Biermann et al. (1967) assumed that the plasma flow rapidly accommodates the new ions, i.e. the entire plasma population can be characterized by a single temperature and flow velocity. This assumption made it possible to apply a single-fluid hydrodynamic treatment for the continuously mass loaded plasma flow and to use the conservation equations to describe the deceleration of the contaminated solar wind flow. Biermann et al. (1967) had also shown that continuous deceleration of the solar wind flow by mass loading is possible only up to a certain point at which the mean molecular weight of the plasma particles reaches a critical value. At this point a weak shock forms and impulsively decelerates the flow to subsonic velocities. Subsequent three-dimensional MHD calculations showed that for Halley class comets a shock wave with Mach number M=2 forms in the upstream plasma flow at a cometocentric distance where the mass addition reaches the following critical value (Schmidt and Wegmann 1982):

$$\frac{\rho u}{\rho_\infty u_\infty} = \frac{\gamma^2}{\gamma^2 - 1} \qquad (1)$$

where γ is the specific heat ratio, ρ and u represent the mass density and flow velocity of the contaminated solar wind flow, while ρ_∞ and u_∞ denote the same quantities in the undisturbed solar wind.

Wallis and Ong (1975) were the first to recognize that implanted cometary ions would not accommodate to the solar wind flow; consequently the application of a single-fluid hydrodynamic treatment was unjustified. By assuming that the flow velocity was perpendicular to magnetic field direction and that the first adiabatic invariant of cometary ions was conserved ($\mu = m_i u^2/2B = \text{const}$, B being the magnetic field magnitude) Wallis and Ong (1975) were able to determine the implanted particle distribution function and combine it with the magnetohydrodynamic equations to obtain the

contaminated solar wind flow parameters. In a subsequent calculation Galeev et al (1985) recognized that cometary ions carry most of the hydrodynamic pressure and that charge exchange cooling of the implanted plasma population can play a very important role in the dynamics of the contaminated solar wind flow.

The first *in situ* observations of a cometary plasma environment (cf. the special issues of **Science** (Vol. 232, pp 353 - 385, April 18, 1986) and **Nature** (Vol. 321, pp 259 - 366, May 15, 1986)) resulted in the detection of very high levels of magnetohydrodynamic turbulence generated by the implanted cometary ion pickup process. These results prompted a whole series of theoretical calculations with varying levels of sophistication attempting to establish the possible presence of various plasmaphysical instabilities in the cometary environment (cf. Galeev 1986, Galeev et al. 1986a., Sagdeev et al. 1986, 1987, Tsurutani and Smith 1986, Buti and Lakhina 1987). There seems to be a general consensus that these strong magnetohydrodynamic waves are generated because the plasma flow velocity is not perpendicular to the interplanetary magnetic field.

Figure 1. is a schematic representation of our present understanding of the pickup geometry. The plot shows a velocity space diagram in the inertial (solar) frame of reference (the V_x axis points towards the sun). V_{SW} and V_c represent the velocities of the solar wind flow and the comet, respectively. It can be seen that the initial velocity of a newly born cometary ion in the solar wind frame of reference is $V_I = V_c - V_{SW}$ (if one neglects the outflow velocity of neutral cometary particles). The dashed line indicates the direction of the interplanetary magnetic field (IMF). The freshly born ion starts to gyrate around the magnetic field line with a magnetic moment of

$$\mu = \frac{m V_{I,\perp}^2}{2 B} \qquad (2)$$

(B is the IMF magnitude and $V_{I,\perp}$ denotes the velocity component perpendicular to the IMF direction) and its guiding center accelerates to a velocity of $V_{I,\perp}$ due to the motional electric field caused by the magnetic field line convection. The result of this process is that newly born particles are distributed along a pickup ring (its projection to the ecliptic is shown in Figure 1). At the same time there is no force to accelerate these particles along field lines, consequently they "inherit" a field aligned velocity of $V_{I\parallel}$. It was shown that this field aligned motion of the pickup ring generates a broad spectrum of magnetohydrodynamic turbulence: as a result of this process strong Alfven waves propagate along the magnetic field lines in both directions (Winske et al. 1985, Galeev 1986, Buti and Lakhina 1987, Sagdeev et al. 1986, 1987, Tsurutani and Smith 1986). In the supersonic, superalfvenic solar wind flow the frequency of the excited waves is much lower than the cyclotron frequency of implanted cometary ions, which in a first approximation interact

with these low frequency Alfven waves without significantly changing their energy (in the solar wind frame of reference). As a result of the rapid wave - particle interaction process the pitch angles of the pickup-ring particles quickly become randomized in the solar wind frame of reference and they become distributed on a shell (having a radius of V_I) around the local solar wind velocity (Gary et al. 1986, Galeev et al. 1986b, Sagdeev et al. 1986, 1987). There is recent experimental indication that this pickup-shell formation is not complete (Mukai et al. 1986, Neugebauer 1986): nevertheless there seems to be a growing consensus in the literature that the distribution of freshly ionized cometary particles can, in fact, be reasonably approximated by a pickup shell in the solar wind frame (cf. Galeev 1986).

Energetic particle measurements at comets Giacobini - Zinner and Halley (Hynds et al. 1986, Ipavich et al. 1986, Somogyi et al. 1986, Kecskeméty et al. 1986, McKenna-Lawlor 1986) detected large fluxes of energetic particles. A significant part of the detected energetic ion population was observed at energies considerably larger than the pickup energy indicating the presence of some kind of acceleration process acting on implanted ions. It was first suggested by Gribov et al. (1986) and Ip and Axford (1986) that second order Fermi acceleration (slow velocity diffusion due to the interaction with propagating Alfven waves) is likely to play an important role in accelerating the implanted cometary ions far upstream from the comets. Ip and Axford applied a simplified diffusion equation to study the potential consequences of this stochastic acceleration process, while Gribov et al. (1986) used a quasilinear technique. Both methods led to similar conclusions: in the solar wind frame of reference at high velocities (well above the ambient flow velocity) the implanted ion distribution function falls off exponentially with an effective temperature, T_v:

$$F(v) \propto \exp\left(-\frac{m v^2}{2 T_v}\right) \qquad (3)$$

Using VEGA magnetic field and plasma observations Gribov et al. (1986) calculated the radial variation of T_v in the unshocked solar wind and compared their results with energetic particle spectra. Even though the model predictions were of the right order of magnitude, the calculated effective temperature profile increased about a factor of 4 faster than the experimental values indicating that simple quasilinear theory is unable to account for the details of the acceleration process. More recently Isenberg (1987b) published an elegant analytic solution to the transport equation describing convection, adiabatic acceleration and velocity diffusion. In order to be able to obtain an analytic solution Isenberg (1987b) neglected the exponential decay factor in the exospheric neutral densities (thus significantly overestimating the implanted ion source) and assumed a prescribed power law deceleration profile for the bulk flow velocity, nevertheless his

solution represents a major step towards self- consistent modeling of the upstream region acceleration of implanted cometary ions.

In this paper a self-consistent, three fluid model of plasma transport and implanted ion acceleration in the unshocked solar wind is presented. The solar wind plasma (assumed to contain only protons and electrons) is depleted by charge exchange with the expanding cometary exosphere, while implanted protons and heavy ions (mainly O^+) are produced by photoionization and charge transfer and lost by charge exchange. A generalized transport equation, describing convection, adiabatic and diffusive velocity change and the appropriate production terms, is used to describe the evolution of the two cometary ion components, while the moments of the Boltzmann equation are used to calculate the solar wind density and pressure. The flow velocity is obtained self-consistently by combining the conservation equations of the three ion species.

Governing equations

It is assumed that the velocity distribution of implanted cometary ions (H^+ and O^+) is isotropic in the solar wind frame due to the rapid pitch-angle scattering by magnetic field turbulence. In this case the phase space density, F, can be expressed as:

$$F = F(t, \vec{x}, v) \tag{4}$$

where t=time, x=position vector, v=random velocity and v=|v|. (Here and throughout the paper three different notations will be used for vectorial quantities: when not marked by coordinate subscripts, vectors are printed boldface in the text or marked by over-arrows in the equations. In the equations written in component notation, summation is implied over coordinate subscripts which occur twice.) The particle transport is described by the following Fokker-Planck equation:

$$\frac{\partial F}{\partial t} + (u_i + v_i)\frac{\partial F}{\partial x_i} - \left(\frac{v_i}{v}\frac{\partial u_i}{\partial t} + \frac{v_i u_j}{v}\frac{\partial u_i}{\partial x_j} + \frac{v_i v_j}{v}\frac{\partial u_i}{\partial x_j}\right)\frac{\partial F}{\partial v} = \frac{\delta F}{\delta t} + \frac{\partial}{\partial v_i}\left(D_{ij}\frac{v_j}{v}\frac{\partial F}{\partial v}\right) \tag{5}$$

where u=mean flow velocity, $\delta F/\delta t$=source term, and D_{ij}=velocity diffusion tensor. In this transport equation spatial diffusion is neglected thus eventually enabling us to reduce the problem to one spatial and one velocity dimension. As it will be pointed out at the end of this paper this simplifying assumption is probably violated and spatial diffusion potentially plays an important role in the upstream region acceleration process. At the same time this assumption makes it possible to consider the effect of second order Fermi acceleration on the implanted ion energy

spectrum in a self-consistent way, thus helping us to delineate the most important physical processes leading to particle energization in the very extended preshock region.

In the present model it is assumed that scattering by the magnetic field turbulence results in rapid isotropization, therefore the velocity diffusion tensor is written in the following form:

$$D_{ij} = D\,\delta_{ij} \tag{6}$$

Using this form the velocity diffusion term in equation (5) becomes:

$$\frac{\partial}{\partial v_i}\left(D_{ij}\frac{v_j}{v}\frac{\partial F}{\partial v}\right) = \frac{1}{v^2}\frac{\partial}{\partial v}\left(D v^2 \frac{\partial F}{\partial v}\right) \tag{7}$$

Here the coefficient D, describes the diffusion of the magnitude of the particle velocity. A simple expression for D was introduced earlier by Fisk (1976) assuming a second order Fermi acceleration process due to interaction with propagating Alfven waves:

$$D = \frac{3}{4}V_A^2\frac{v}{L} \tag{8}$$

where L=Fermi scattering mean free path and the Alfven velocity can be expressed as

$$V_A^2 = \frac{B^2}{4\pi\rho_{ion}} \tag{9}$$

ρ_{ion} being the total ion mass density. The Fisk (1976) approximation was used by Ip and Axford (1986) to investigate the potential importance of the second order Fermi acceleration at comets: they assumed that due to the strong scattering process the mean free path, L, was approximately equal to the ion gyroradius, r_c. Recently a more sophisticated approach was adopted by Isenberg (1987b) who used the quasilinear approximation (Isenberg 1987a) to obtain the following velocity diffusion coefficient:

$$D = \frac{\pi}{\gamma(\gamma+2)}V_A^2\left(\frac{Ze}{mc}\right)^2 P_0\left(\frac{2\pi f_0}{\Omega}\right)^{\gamma}\left(\frac{v}{u}\right)^{\gamma-1} \tag{10}$$

where Ze, m and Ω represent the particle charge, mass and gyrofrequency, respectively. The observed magnetic field frequency power spectrum, P, was approximated with the following expression above a critical frequency, f_0:

$$P(f) = P_0\left(\frac{f}{f_0}\right)^{-\gamma} \tag{11}$$

Here P_0 is the magnetic field wave power at the frequency, f_0. It can be seen that by substituting a $\gamma=1$ value to equation (10) one obtains a velocity independent diffusion coefficient which corresponds to a Fermi scattering mean free path of

$$\frac{L}{r_c} = \frac{9}{8\pi^2 f_0}\frac{B^2}{P_0} \tag{12}$$

Substituting more or less typical parameter values observed in the comet Halley upstream region (Acuna et al. 1986) one obtains that for heavy implanted ions the mean free path (L/r_c) decreases from several hundred (in the free streaming solar wind) to approximately 10 just at the bow shock. In any case the Fermi scattering mean free path seems to be much larger than unity, consequently Ip and Axford (1986) probably overestimated the significance of this process in their simple diffusion calculation.

The $\delta F/\delta t$ term in the Fokker-Planck equation (eq. 5) describes the photoionization and charge exchange of neutral particles, as well as the charge exchange loss of ions.When deriving these terms it was assumed that the orbital velocity of the comet was much smaller than the plasma flow velocity; this assumption is valid in the upstream solar wind and only breaks down in the stagnation region well behind the shock. It was also assumed that implanted protons do not contribute to the solar wind population (in other words the pickup H^+ ions do not become thermalized in the vicinity of the comet). The solar wind source term with these simplifications becomes

$$\frac{\delta F_{sw}}{\delta t} = -\left|\vec{u}+\vec{v}\right|\frac{F_{sw}}{\lambda_p} \tag{13}$$

The source terms of the implanted proton and heavy ion populations are:

$$\frac{\delta F_p}{\delta t} = \delta^3(\vec{u}+\vec{v})\frac{n_H}{\tau_H} - \left|\vec{u}+\vec{v}\right|\frac{F_p}{\lambda_p} \tag{14}$$

$$\frac{\delta F_h}{\delta t} = \delta^3(\vec{u}+\vec{v})\frac{n_O}{\tau_O} - \left|\vec{u}+\vec{v}\right|\frac{F_h}{\lambda_h} \tag{15}$$

where n_H and n_O represent the neutral hydrogen and heavy particle (mainly oxygen) densities, respectively. The charge transfer mean free paths of the protons and heavy ions are defined as

$$\frac{1}{\lambda_p} = \sigma_{pH} n_H + \sigma_{pO} n_O \tag{16}$$

$$\frac{1}{\lambda_h} = \sigma_{hH} n_H + \sigma_{hO} n_O \tag{17}$$

Here σ_{pH}, σ_{pO}, σ_{MH}, and σ_{hO} represent the proton - hydrogen, proton - oxygen, heavy ion - hydrogen and heavy ion - oxygen charge transfer cross sections, respectively. The ionization lifetimes are defined as

$$\frac{1}{\tau_H} = \frac{1}{\tau_{H,photo}} + \frac{1}{\tau_{H,ct}} \tag{18}$$

$$\frac{1}{\tau_O} = \frac{1}{\tau_{O,photo}} + \frac{1}{\tau_{O,ct}} \tag{19}$$

where $\tau_{H,photo}$ and $\tau_{O,photo}$ represent the photoionization lifetimes, while the the neutral particle lifetimes for charge exchange are defined as

$$\frac{1}{\tau_{H,ct}} = \sigma_{pH}\left[I^{(0)}_{SW} + I^{(0)}_{p}\right] + \sigma_{hH} I^{(0)}_{h} \tag{20}$$

$$\frac{1}{\tau_{O,ct}} = \sigma_{pO}\left[I^{(0)}_{SW} + I^{(0)}_{p}\right] + \sigma_{hO} I^{(0)}_{h} \tag{21}$$

The $I^{(0)}$ function describes the average ion flux with respect of the neutral particles and is defined in Appendix A.

The $\delta^3(u+v)$ multiplication factor in equations (14) and (15) expresses the fact that right after ionization the new particles are at rest and their accommodation to the flow requires the redistribution of the available momentum and energy. By using this source term it is implicitly assumed that the newly born ions instantaneously form a shell distribution, otherwise (14) and (15) would violate our assumption about the form of the distribution function (equation 4).

The generalized implanted ion transport equation is obtained from the Fokker-Planck equation (eq. 5) by averaging over the velocity space angular distribution (i.e. by applying the integral operator

$$\frac{1}{4\pi}\int d\Omega_v$$

to eq. 5):

$$\frac{\partial F}{\partial t} + u_i\frac{\partial F}{\partial x_i} - \frac{v}{3}\frac{\partial u_i}{\partial x_i}\frac{\partial F}{\partial v} = \frac{1}{v^2}\frac{\partial}{\partial v}\left(D v^2\frac{\partial F}{\partial v}\right) - \frac{G}{\lambda} u F + \delta(u-v)\frac{n_n}{4\pi\tau v^2} \tag{22}$$

Here n_n represents the appropriate neutral density (hydrogen or oxygen), λ is the charge exchange mean free path and

$$G(u,v) = \begin{cases} \left(1 + \frac{v^2}{3u^2}\right) & u > v \\ \frac{v}{u}\left(1 + \frac{u^2}{3v^2}\right) & u \le v \end{cases} \tag{25}$$

This transport equation (eq. 22) was applied to the two implanted ion species, while the overall flow characteristics were obtained by calculating the moments of the original Fokker-Planck equation (eq. 5). By applying the $\int dv$, $\int dv v_i$, and $\int dv v^2$ operators one obtains the following continuity, momentum and energy equations:

$$\frac{\partial n}{\partial t} + u_i \frac{\partial n}{\partial x_i} + n \frac{\partial u_i}{\partial x_i} = \frac{n_n}{\tau} - \frac{I^{(0)}}{\lambda} \tag{24}$$

$$m n \frac{\partial u_i}{\partial t} + m n u_j \frac{\partial u_i}{\partial x_j} + \frac{\partial p}{\partial x_i} = - m u_i \frac{n_n}{\tau} - m u_i \frac{I^{(1)}}{\lambda} \tag{25}$$

$$\frac{\partial p}{\partial t} + u_i \frac{\partial p}{\partial x_i} + \frac{5}{3} p \frac{\partial u_i}{\partial x_i} = \frac{m}{3} \mathcal{D}_0 \mathcal{P}_\gamma + \frac{m}{3} u^2 \frac{n_n}{\tau} - \frac{m}{3} u^2 \frac{I^{(2)}}{\lambda} \tag{26}$$

The functions $I^{(0)}$, $I^{(1)}$, $I^{(2)}$ and $\mathcal{P}_\gamma$ are defined in Appendix A, while the quantity $\mathcal{D}_0$ is given by:

$$\mathcal{D}_0 = \frac{\pi}{\gamma(\gamma+2)} V_A^2 \left(\frac{Ze}{mc}\right)^2 P_0 \left(\frac{2\pi f_0}{\Omega}\right)^\gamma \left(\frac{1}{u}\right)^{\gamma-1} \tag{27}$$

It should be noted that there is no velocity diffusion of solar wind ions ($\mathcal{D}_{0,sw}=0$).

Adding the three continuity, momentum and energy equations one obtains:

$$\frac{\partial \rho_{ion}}{\partial t} + \frac{\partial}{\partial x_i}\left(u_i \rho_{ion}\right) = \frac{\rho_H}{\tau_H} + \frac{\rho_O}{\tau_O} - \frac{m_p}{\lambda_p}\left(I_{sw}^{(0)} + I_p^{(0)}\right) - \frac{m_h}{\lambda_h} I_h^{(0)} \tag{28}$$

$$\rho_{ion} \frac{\partial u_i}{\partial t} + \rho_{ion} u_j \frac{\partial u_i}{\partial x_j} + \frac{\partial p_{ion}}{\partial x_i} = - u_i \left[\frac{\rho_H}{\tau_H} + \frac{\rho_O}{\tau_O} + \frac{m_p}{\lambda_p}\left(I_{sw}^{(1)} + I_p^{(1)}\right) + \frac{m_h}{\lambda_h} I_h^{(1)}\right] \tag{29}$$

$$\frac{\partial p_{ion}}{\partial t} + u_i \frac{\partial p_{ion}}{\partial x_i} + \frac{5}{3} p_{ion} \frac{\partial u_i}{\partial x_i} = \frac{1}{3}\left(m_p \mathcal{D}_{0,p} \mathcal{P}_{\gamma,p} + m_h \mathcal{D}_{0,h} \mathcal{P}_{\gamma,h}\right) + \frac{u^2}{3}\left[\frac{\rho_H}{\tau_H} + \frac{\rho_O}{\tau_O} - \frac{m_p}{\lambda_p}\left(I_{sw}^{(2)} + I_p^{(2)}\right) - \frac{m_h}{\lambda_h} I_h^{(2)}\right] \tag{30}$$

where the total mass density and pressure are defined as

$$\rho_{ion} = \rho_{sw} + \rho_p + \rho_h \tag{31}$$

$$p_{ion} = p_{sw} + p_p + p_h \tag{32}$$

In a steady-state case the upstream region momentum and energy equations can be combined to yield

$$\frac{du}{ds} = \frac{1}{3\rho_{ion}u^2 - 5p_{ion}} \left\{5 p_{ion} u \frac{A'}{A} - D_F - W - 4u^2\left(\frac{\rho_H}{\tau_H} + \frac{\rho_O}{\tau_O}\right)\right\} \tag{33}$$

where s is the pathlength along the plasma flow lines, A(s)=flow area function, A'=dA/ds and

$$D_F = m_p \mathcal{D}_{0,p} \mathcal{P}_{\gamma,p} + m_h \mathcal{D}_{0,h} \mathcal{P}_{\gamma,h} \tag{34}$$

$$W = u^2 \frac{m_p}{\lambda_p}\left[\left(3 I_{sw}^{(1)} - I_{sw}^{(2)}\right) + \left(3 I_p^{(1)} - I_p^{(2)}\right)\right] + u^2 \frac{m_h}{\lambda_h}\left(3 I_h^{(1)} - I_h^{(2)}\right) \tag{35}$$

In our model it is assumed that the solar wind particles follow a Maxwellian velocity distribution, while the implanted ions in the plasma frame of reference are described by an isotropic distribution function, consequently the steady state solar wind is described by the following fluid equations (it should be noted that the flow velocity is determined by equation (33)):

$$\frac{dn_{sw}}{ds} = - n_{sw} \frac{A'}{A} - \frac{n_{sw}}{u} \frac{du}{ds} - \frac{I_{sw}^{(0)}}{u \lambda_p} \tag{36}$$

$$\frac{dp_{sw}}{ds} = - \frac{5}{3} p \frac{A'}{A} - \frac{5}{3} \frac{p_{sw}}{u} \frac{du}{ds} - \frac{u}{3} m_p \frac{I_{sw}^{(2)}}{\lambda_p} \tag{37}$$

The implanted ion transport equations are:

$$\frac{\partial F_p}{\partial s} = \frac{D_p}{u}\frac{\partial^2 F_p}{\partial v^2} + \left[\frac{v}{3}\frac{A'}{A} + \frac{v}{3}\frac{1}{u}\frac{du}{ds} + \frac{2D_p}{uv} + \frac{1}{u}\frac{\partial D_p}{\partial v}\right]\frac{\partial F_p}{\partial v} - \frac{G}{\lambda_p}F_p + \frac{n_H\,\delta(u-v)}{4\pi\,\tau_H\,u\,v^2} \quad (38)$$

$$\frac{\partial F_h}{\partial s} = \frac{D_h}{u}\frac{\partial^2 F_h}{\partial v^2} + \left[\frac{v}{3}\frac{A'}{A} + \frac{v}{3}\frac{1}{u}\frac{du}{ds} + \frac{2D_h}{uv} + \frac{1}{u}\frac{\partial D_h}{\partial v}\right]\frac{\partial F_h}{\partial v} - \frac{G}{\lambda_h}F_h + \frac{n_O\,\delta(u-v)}{4\pi\,\tau_O\,u\,v^2} \quad (39)$$

Results and discussion

In the present set of model calculations equations (33) and (36-39) were solved simultaneously using an implicit Crank-Nicolson method. In order to do this we also had to define a neutral exosphere and a magnetic field turbulence power spectrum model. For the neutral densities the following expressions were used

$$n_O = \frac{Q_O}{4\pi r^2 V_O}\exp\left(-\int_{R_c}^{r} dr\,\frac{1}{V_O\,\tau_O}\right) \quad (40)$$

$$n_H = \frac{2Q_O}{4\pi r^2 V_H}\exp\left(-\int_{R_c}^{r} dr\,\frac{1}{V_H\,\tau_H}\right)\left\{1 - \exp\left(-\frac{r}{\lambda_{diss}}\right)\right\} \quad (41)$$

Here Q_O is the neutral oxygen production rate (it is assumed that the comet is water dominated, therefore $Q_O=Q_{H2O}$), V_O and V_H are the O and H exospheric radial velocities, while λ_{diss} is an average molecular dissociation scalelength producing hydrogen and heavy neutral particles. The factor of 2 in eq. (41) comes from the assumption that the comet originally produces water vapor molecules which eventually dissociate to two H and one O atoms. In the present calculations $Q_O=10^{30}$ molecules/s, $\lambda_{diss}=2\times10^6$ km, $V_O=1$ km/s, and $V_H=10$ km/s values were adopted based upon comet Halley observations (cf. the special issue of **Nature** (Vol. 321, pp 259 - 366, May 15, 1986) and the proceedings of the Heidelberg comet symposium (**Proc. 20th ESLAB Symposium on the Exploration of Halley's Comet** (eds. B. Battrick, E.J. Rolfe and R. Reinhard), ESA SP-250, Vol. 1-3, 1986)). The τ_H and τ_O quantities were calculated using equations (18) and (19) with the following parameter values:

$$\sigma_{pH} = \sigma_{pO} = \sigma_{hH} = \sigma_{hO} = 1\times10^{-15}\,cm^2$$

$$\tau_{H,photo} = 1.11\times10^7\,d^2 \text{ seconds}$$

$$\tau_{O,photo} = 4.05\times10^6\,d^2 \text{ seconds}$$

where d is the heliocentric distance in AUs.

Based on VEGA-1 and -2 observations Galeev et al. (1986b) showed that the energy density of excited Alfven waves increases exponentially as one approaches the comet. It was also shown by Galeev et al. (1986b) that the characteristic scalelength of this exponential increase is approximately the same as the exospheric neutral ionization scalelength. At the same time the GIOTTO magnetometer results (Acuna et al. 1986) indicate that at a cometocentric distance of $\sim1.5\times10^6$ km the power level of the magnetic field turbulence was about $P_0=(30\div60)\,\gamma^2$/Hz near the heavy ion gyrofrequency ($\Omega_0=2\pi f_0=ZeB/m_Oc$). On the other hand observations at comets Giacobini - Zinner and Halley (Tsurutani and Smith 1986, Acuna et al. 1986) showed a magnetic field spectral index of $\gamma=5/3$. On the basis of these measurements and theoretical considerations (Galeev 1986) the power level of the magnetic field turbulence is approximated by the following expression:

$$P_0 = P_{0,\infty} + P_{0,implant}\left(\frac{\rho_{ion}\,u}{\rho_{ion,\infty}\,u_\infty} - 1\right) \quad (42)$$

where $P_{0,\infty}$ is the wave power of ambient fluctuations in the solar wind under average conditions, while the wave power generated by the pickup process can be approximated as (cf. Galeev 1986)

$$P_{0,implant} = \frac{1}{2}\rho_{ion,\infty}\,u_\infty\,V_A\,\frac{1}{\Omega_0} \quad (43)$$

In the present calculations a constant magnetic field magnitude of $B=10\gamma$ was adopted in the unshocked flow, while the ambient fluctuation level was assumed to be $P_{0,\infty}=5\,\gamma^2$/Hz.

Equations (33) and (36-39) were solved simultaneously in the unshocked plasma flow along flow lines parallel to the sun - comet line. In this region the change of the flow tube cross sectional area (the area delimited by specific streamlines) is not very important (cf. Wallis and Ong 1975, Galeev et al. 1985), therefore the A'/A terms were neglected. The initial condition described an undisturbed solar wind flow ($u_{sw,\infty}=500$ km/s, $n_{sw,\infty}=10$ cm^{-3}, $T_{sw,\infty}=10^5$ K) at an distance of 10^7 km upstream along the flow line with no implanted ions. The partial differential equation system was solved using a fixed spatial step size of 100 km and a velocity space grid size of 10

km/s: 1000 grid points were used to describe the implanted H^+ distribution function, while the O^+ distribution was characterized by 300 points. The boundary conditions were

$$F(t, \vec{x}, v=\infty) = 0 \qquad (44)$$

and

$$\left.\frac{\partial F(t, \vec{x}, v)}{\partial v}\right|_{v=0} = 0 \qquad (45)$$

In other words the distribution function vanishes for very large velocities and there is no velocity gradient across the v=0 point. The calculation was stopped when the flow Mach number decreased to a value of 2, where three dimensional MHD calculations predicted the formation of a weak shock (cf. Schmidt and Wegmann 1982).

Figure 2. shows the variation of the implanted ion velocity diffusion coefficients (for a velocity of v=u), the diffusion mean free path and the magnetic field power (at a reference frequency of f_0=0.01Hz) along the subsolar streamline. It can be easily seen that the mean free path of the second order Fermi acceleration decreases dramatically as one approaches the comet. The power of the magnetic field turbulence starts to exceed the interplanetary level at around 2×10^6 km upstream of the comet and reaches about 200 γ^2/Hz at the shock. Figure 3. shows the variation of the exospheric neutral densities, charge exchange mean free path and ionization lifetimes along the same subsolar flow line. Inspection of Figure 3. reveals that the ionization lifetime of neutral hydrogen and oxygen is fairly constant along the stream line and its value is determined to a large extent by the charge transfer cross section between the cometary neutrals and solar wind ions (the photoionization lifetimes are much larger than the values shown in Figure 3). The charge exchange scalelength decreases from 10^{11} km at a distance of 10^7 km to about 10^7 km near the "shock" (defined as the M=2 point). This means that even though the charge loss of ions is fairly insignificant, it represents a sizable contribution to the ionization source.

Figure 4. shows the plasma flow deceleration along the subsolar flow line due to various processes. It can be seen that beyond ~6×10^6 km the most of the deceleration is caused by the H^+ mass loading, while closer to the comet the O^+ mass addition is the major deceleration source. It is interesting to note that near the shock wave the implanted O^+ loss and H^+ mass addition are causing comparable decelerations. Figure 5. shows the the flow velocity, Mach number, particle number density and pressure along the subsolar flow line. Inspection of Figure 5. shows that the flow velocity does not show any significant change beyond ~2×10^6 km, while the Mach number starts to decrease much earlier due to the increase of the total pressure. It should be noted that even

though in the vicinity of the shock the plasma pressure is dominated by the heavy implanted ion pressure, the implanted ion concentration never exceeds a few percent of the total plasma density in the unshocked flow. This result of the present numerical simulation is a good justification of the basic assumption used in an earlier paper (Galeev et al. 1985).

Figures 6. and 7. show the evolution of the implanted H^+ and O^+ distributions along the subsolar flow line. The plots show four "snapshots" at 7×10^6 km, 4×10^6 km, 1×10^6 km and the "bow shock" (located at a cometocentric distance of 0.37×10^6 km). Inspection of Figures 6 and 7 reveals that the distribution functions peak at the local plasma flow velocity and rapidly decrease to both directions. The high energy tail of the distribution function can be well approximated by an exponential as predicted by several previous papers (cf. Ip and Axford 1986, Gribov et al. 1986, Isenberg 1987b). Figure 8. shows the variation of the effective asymptotic temperature of the O^+ distribution function along the subsolar flow line (in order to achieve easy comparison with the temperature values derived from the Tünde experiment onboard the VEGA spececraft the asymptotic temperature is defined in this paper as the average slope of the O^+ distribution function between 100 and 120 keV). It can be seen that this "scaling" temperature gradually increases up to about 1.5×10^6 km, when a rapid "heating" takes place due to the exponentially increasing magnetic field turbulence level.

Figures 9. and 10. exhibit snapshots of calculated implanted ion distributions along the VEGA-1 trajectory. These distributions behave quite similarly to those calculated for the subsolar stream lines with one notable difference: now the magnitudes are about two orders of magnitude smaller at the bow shock than along the subsolar flow line. This fact is quite understandable because there is much less mass addition along flow lines not passing through the the dense inner coma region, consequently there are much fewer particles to accelerate to higher energies. Figure 11. shows the calculated O^+ effective temperature along the VEGA-1 trajectory together with the observed values (Kecskeméty et al. 1987): the agreement seems to be quite remarkable. It should be noted that an analogous effective temperature profile was calculated by Gribov et al. (1986) combining a quasilinear approximation with VEGA particles and fields measurements: they predicted a much faster than observed increase of the temperature profile along the VEGA trajectory.

The observed VEGA-1 distribution at the comet Halley bow shock (Kecskeméty et al. 1987) is shown in both Figures 7. and 10. A simple comparison of the these values reveals that there is a significant discrepancy between the measured and calculated values for the VEGA trajectory. This discrepancy is probably a result of the neglect of the spatial transport of implanted

ions along magnetic field lines: in the present one dimensional calculation this potentially important effect was not taken into account. As the shape of the implanted ion distributions evolves quite similarly along different flow lines (because the shape of the distribution function is mainly determined by the magnetic field fluctuation level in the mildly disturbed solar wind, where most of the Fermi acceleration takes place), the neglect of field aligned transport mainly results in an uncertainty of the magnitude of the distribution function, while the effective temperatures seem to be fairly insensitive to the presence of spatial diffusion.

Summary

In this paper a self-consistent three-component model of plasma transport and implanted ion acceleration in the preshock region was presented. The ambient solar wind plasma was treated as a fluid, while the implanted cometary ions (H^+ and O^+) were described by Fokker-Planck transport equations. The physical model assumed that solar wind particles follow a Maxwellian distribution drifting with a gradually decreasing flow velocity and are lost by charge exchange with cometary neutrals. The implanted ions are continuously created by photoionization and charge exchange of the cometary neutrals and lost by charge transfer. The model assumes that spatial transport is dominated by convection (spatial diffusion effects are neglected in the present approximation) and that implanted ions undergo fast pitch angle isotropization (in the solar wind frame of reference) and a much slower velocity diffusion process caused by second order Fermi scattering on propagating Alfven waves.

The coupled hydrodynamic - kinetic transport equation system was numerically solved for conditions similar to those in the preshock region of comet Halley during the VEGA-1 encounter. The results indicate that second order Fermi acceleration is probably the main source of implanted particle acceleration in the unshocked solar wind. There is also indication that in addition to Fermi acceleration field aligned transport of implanted ions may also play an important role in determining the energetic particle fluxes in the vicinity of comets.

Acknowledgements

The author is grateful to Ms. Kinga Lorencz for her valuable contribution to this work. Useful discussions with Drs. T.E. Cravens, K. Kecskeméty and A. Körösmezey are also acknowledged. This work was supported by NSF grants AST-8605994, ATM-8508753 and NASA grant NGR 23-005-015. Acknowledgements are also made to the University of Michigan and to the National Center for Atmospheric Research sponsored by NSF, for the computing time used in this research.

References

Acuna, M.H., Glassmeier, K.H., Burlaga, L.F., Neubauer, F.M., and Ness, N.F., Upstream waves of cometary origin detected by the GIOTTO magnetic field experiment, in **Proc. 20th ESLAB Symposium on the Exploration of Halley's Comet** (eds. B. Battrick, E.J. Rolfe and R. Reinhard), ESA SP-250, Vol. 3., p. 447, 1986.

Buti, B., and Lakhina, G.S., Stochastic acceleration of cometary ions by lower hybrid waves, **Geophys. Res. Lett., 14**, 1987.

Biermann, L. Brosowski, B., and Schmidt, H.U., The interaction of the solar wind with a comet, **Solar Physics, 1**, 254, 1967.

Fisk, L.A., On the acceleration of energetic particles in the interplanetary medium, **J. Geophys. Res., 81**, 4641, 1976.

Gary, S.P., Hinata, S., Madland, C.D., and Winske, D., The development of shell-like distributions from newborn cometary ions, **Geophys. Res. Lett., 13**, 1364, 1986.

Galeev, A.A., Theory and observations of solar wind/cometary plasma interaction processes, in **Proc. 20th ESLAB Symposium on the Exploration of Halley's Comet** (eds. B. Battrick, E.J. Rolfe and R. Reinhard), ESA SP-250, Vol. 1., p.3, 1986.

Galeev, A.A., Cravens, T.E., and Gombosi, T.I., Solar wind stagnation near comets, **Astrophys. J., 289**, 807, 1985.

Galeev, A.A., Gribov, B.E., Gombosi T., Gringauz, K.I., Klimov, S.I., Oberz, P., Remizov, A.P., Riedler, W., Sagdeev, R.Z., Savin, S.P., Sokolov, A.Yu., Shapiro, V.D., Shevchenko, V.I., Szegö, K., Verigin, M.I., end Yeroshenko, Ye.G., Position and structure of the comet Halley bow shock: Vega-1 and Vega-2 measurements, **Geophys. Res. Lett., 13**, 841, 1986a.

Galeev, A.A., Sagdeev, R.Z., Shapiro, V.D., Shevchenko, V.I., and Szegö, K., Mass loading and MHD turbulence in the solar wind/comet interaction region, in **Proc. of the Joint Varenna - Abastumani International School & Workshop on "Plasma Astrophysics"**, ESA SP-251, p. 307, 1986b.

Gombosi T.I., Nagy A.F., and Cravens T.E.: Dust and neutral gas modeling of the inner atmospheres of comets, **Reviews of Geophysics, 24**, 667, 1986.

Gribov, B.E., Kecskeméty, K., Sagdeev, R.Z., Shapiro, V.D., Shevchenko, V.I., Somogyi A.J., Szegö, K., Erdös, G., Eroshenko, E.G., Gringauz, K.I., Keppler, E., Marsden R., Remizov, A.P., Richter, A.K., Riedler, W., Schwingenschuh, K., and Wenzel, K.P., Stochastic Fermi acceleration of ions in the pre-shock region of comet Halley, in **Proc. 20th ESLAB Symposium on the Exploration of Halley's Comet** (eds. B. Battrick, E.J. Rolfe and R. Reinhard), ESA SP-250, Vol. 1., p. 271, 1986.

Gringauz K.I., Gombosi T.I., Remizov A.P., Apáthy I., Szemerey I., Verigin M.I., Denchikova L.I., Dyachkov A.V., Keppler E., Klimenko I.N., Richter A.K., Somogyi A.J., Szegö K., Szendrö S., Tátrallyay M., Varga A., Vladimirova G.A.: First in situ plasma and neutral gas measurements at comet Halley: initial VEGA results, **Nature, 321**, 282, 1986a.

Gringauz K.I., Gombosi T.I., Remizov A.P., Apáthy I., Szemerey I., Verigin M.I., Denshchikova L.I., Dyachkov A.V., Keppler E., Klimenko I.N., Richter A.K., Somogyi A.J., Szegö K., Szendrö S., Tátrallyay M., Varga A., Vladimirova G.A.: First results of plasma and neutral gas measurements from VEGA-1/2 near comet Halley, **Advances in Space Research, 5**(12), 165, 1986b.

Hynds, R.J., Cowley, S.W.H., Sanderson, T.R., Wenzel, K.P., and van Rooijen, J.J., Observations of energetic ions from comet Giacobini - Zinner, **Science, 232**, 361, 1986.

Ip, W.-H., and Axford, W.I., The acceleration of particles in the vicinity of comets, preprint, MPAE-W-100-86-07, 1986.

Ipavich, F.M., Galvin, A.B., Gloeckler, G., Hovestadt, D., Klecker, B., and Scholer, M., Comet Giacobini - Zinner: In situ observations of energetic heavy ions, **Science, 232**, 366, 1986.

Isenberg, P.A., Evolution of interstellar pickup ions in the solar wind, **J. Geophys. Res., 92**, 1067, 1987a.

Isenberg, P.A., Energy diffusion of pickup ions upstream of comets, **J. Geophys. Res.**, submitted, 1987b.

Kecskeméty K., Cravens T.E., Afonin V.V., Erdös G., Eroshenko E.G., Gan L., Gombosi T.I., Gringauz K.I., Keppler E., Klimenko I.N., Marsden R.G., Nagy A.F., Remizov A.P., Richter A.K., Riedler W., Schwingenschuh K., Somogyi A.J., Szegö K., Tátrallyay M., Varga A., Verigin M.I., Wenzel K.P., Energetic pick-up ions outside the comet Halley bow shock, in **Proc. 20th ESLAB Symposium on the Exploration of Halley's Comet** (eds. B. Battrick, E.J. Rolfe and R. Reinhard), ESA SP-250, Vol. 1, p. 109, 1986.

Kecskeméty K., Cravens T.E., Afonin V.V., Erdös G., Eroshenko E.G., Gan L., Gombosi T.I., Gringauz K.I., Keppler E., Klimenko I.N., Marsden R.G., Nagy A.F., Remizov A.P., Richter A.K., Riedler W., Schwingenschuh K., Somogyi A.J., Szegö K., Tátrallyay M., Varga A., Verigin M.I., Wenzel K.P., Pick-up ions in the unshocked solar wind at comet Halley, **J. Geophys. Res.**, submitted, 1987.

McKenna-Lawlor, S., Kirsch, E., O'Sullivan, D., Thompson, A., and Wenzel, K.P., Energetic ions in the environment of comet Halley, **Nature, 321**, 347, 1986.

Mukai, T., Miyake, W., Terasawa, T., Kitayama, M., Hirao, K., Plasma observation by Suisei of solar wind interaction with comet Halley, **Nature, 321**, 299, 1986.

Remizov A.P., Verigin M.I., Gringauz K.I., Apáthy I., Szemerey I., Gombosi T.I., Richter A.K., Measurements of neutral particle density in the vicinity of comet Halley by Plasmag-1 on board VEGA-1 and VEGA-2, in **Proc. 20th ESLAB Symposium on the Exploration of Halley's Comet** (eds. B. Battrick, E.J. Rolfe and R. Reinhard), ESA SP-250, Vol. 1, p. 387, 1986.

Sagdeev, R.Z., Shapiro, V.D., Shevchenko, V.I., and Szegö, K., MHD turbulence in the solar wind - comet interaction region, **Geophys. Res. Lett., 13**, 85, 1986.

Sagdeev, R.Z., Shapiro, V.D., Shevchenko, V.I., and Szegö, K., The effect of mass loading outside cometary bow shock for the plasma and wave measurements in the coming cometary missions, **J. Geophys. Res., 92**, 1131, 1987.

Schmidt, H.U., and Wegmann, R., Plasma flow and magnetic fields in comets, in **Comets** (ed. L.L. Wilkening), Univ. of Arizona Press, Tucson, p. 538, 1982.

Somogyi A.J., Gringauz K.I., Szegö K., Szabó L., Kozma Gy., Remizov A.P., Erö J., Klimenko I.N., T.-Szücs I., Verigin M.I., Windberg J., Cravens T.E., Dyachkov A.V., Erdös G., Faragó M., Gombosi T.I., Kecskeméty K., Keppler E., Kovács T., Kondor A., Logachev Yu.I., Lohonyai L., Marsden R., Redl R., Richter A.K., Stolpovskii V.G., Szabó J., Szentpétery I., Szepesváry A., Tátrallyay M., Varga A., Wenzel K.P., Vladimirova G.A., Zarándy A.: First observations of energetic particles near comet Halley, **Nature, 321**, 285, 1986.

Tsurutani, B.T., and Smith, E.J., Strong hydromagnetic turbulence associated with comet Giacobini - Zinner, **Goephys. Res. Lett., 13**, 259, 1986.

Wallis, M.K., and Ong, R.S.B., Strongly cooled ionizing plasma flows with applications to Venus, **Planet. Space Sci., 23**, 713, 1975.

Winske D., Wu, C.S., Li, Y.Y., Mou Z.Z., and Guo S.Y., Coupling of newborn ions to the solar wind by electromagnetic instabilities and their interaction with the bow shock, **J. Geophys. Res., 90**, 2713, 1985.

Appendix A
Some quantities related to the moments of the distribution function

It can be shown that

$$\int d\Omega_v \, v_i = 0 \tag{A1}$$

$$\int d\Omega_v \, v_i v_j = \frac{4\pi}{3} v^2 \delta_{ij} \tag{A2}$$

$$\int d\Omega_v \, v_i v_j v_k = 0 \tag{A3}$$

$$\int d\Omega_v \, v_i v_j v_k v_l = \frac{4\pi}{3} v^4 (\delta_{ij}\delta_{kl} + \delta_{ik}\delta_{jl} + \delta_{il}\delta_{jk}) \tag{A4}$$

Based on the non-vanishing moments of the distribution function the following quantities can be defined:

$$n(t,\vec{x}) = 4\pi \int_0^\infty dv \, v^2 F(t, \vec{x}, v) \tag{A5}$$

$$p(t, \vec{x}) = \frac{4\pi}{3} m \int_0^\infty dv \, v^4 F(t, \vec{x}, v) \tag{A6}$$

$$q(t,\vec{x}) = \frac{4\pi}{15} m \int_0^\infty dv \, v^6 F(t, \vec{x}, v) \tag{A7}$$

By using the simple identity

$$\int_0^\infty dv \, v^s \frac{\partial F}{\partial v} = -s \int_0^\infty dv \, v^{s-1} F \tag{A8}$$

the following relation can be obtained

$$\mathcal{P}_\gamma = 4\pi \int_0^\infty dv \, v^2 \frac{\partial}{\partial v}\left(v^{1+\gamma} \frac{\partial F}{\partial v} \right) = 8\pi (\gamma + 2) \int_0^\infty dv \, v^{1+\gamma} F \tag{A9}$$

The charge exchange related loss terms can be expressed as

$$I^{(0)} = \int d\Omega_v \int_0^{\infty} dv\, v^2 \left|\vec{u} + \vec{v}\right| F(t, \vec{x}, v) = u\, n + \frac{p}{u\, m} - M_4 + 3M_3 - 3M_2 + M_1 \quad (A.0)$$

$$I^{(1)} = \int d\Omega_v \int_0^{\infty} dv\, v^2 \frac{\vec{u}\cdot\vec{v}}{u^2} \left|\vec{u} + \vec{v}\right| F(t, \vec{x}, v) = \frac{p}{u\, m} - \frac{q}{u^3 m} + \frac{M_6}{5} - M_4 + M_3 - \frac{M_1}{5} \quad (A.1)$$

$$I^{(2)} = \int d\Omega_v \int_0^{\infty} dv\, v^2 \frac{v^2}{u^2} \left|\vec{u} + \vec{v}\right| = \frac{3\, p}{u\, m} + \frac{5\, q}{u^3 m} - M_6 + 3M_5 - 3M_4 + M_3 \quad (A.2)$$

where

$$M_k(t, \vec{x}, u) = \frac{4\pi}{3\, u^{k-3}} \int_u^{\infty} dv\, v^k F(t, \vec{x}, v) \quad (A.3)$$

Appendix B
Moments of the Maxwellian distribution

In this case the distribution function is

$$F(t, \vec{x}, v) = \frac{n}{V_0^3 \pi^{3/2}} \exp\left(-\frac{v^2}{V_0^2}\right) \quad (B1)$$

where

$$V_0 = \sqrt{\frac{2\, p}{m\, n}} \quad (B2)$$

The fourth moment of the distribution function now can be expressed as

$$q = \frac{p^2}{m\, n} \quad (B3)$$

Introducing the following dimensionless quantity

$$x_0 = \frac{u}{V_0} \quad (B4)$$

one can calculate the M_k quantities

$$M_0 = \frac{2}{3} n\, u\, x_0^2 \left[1 - \mathrm{erf}(x_0)\right] \quad (B5)$$

$$M_1 = \frac{2}{3\sqrt{\pi}} n\, u\, x_0\, e^{-x_0^2} \quad (B6)$$

$$M_2 = \frac{M_0}{2\, x_0^2} + M_1 \quad (B7)$$

$$M_3 = \left(1 + \frac{1}{x_0^2}\right) M_1 \quad (B8)$$

$$M_4 = \frac{3}{4} \frac{M_0}{x_0^4} + \left(1 + \frac{3}{2\, x_0^2}\right) M_1 \quad (B9)$$

$$M_5 = \left(1 + \frac{2}{x_0^2} + \frac{2}{x_0^4}\right) M_1 \tag{B10}$$

$$M_6 = \frac{15}{8}\frac{M_0}{x_0^6} + \left(1 + \frac{5}{2x_0^2} + \frac{15}{4x_0^4}\right) M_1 \tag{B11}$$

The charge exchange loss functions:

$$I^{(0)} = \left(u\,n + \frac{p}{u\,m}\right) \mathrm{erf}(x_0) + \frac{1}{\sqrt{\pi}}\, n \left(\frac{2p}{m\,n}\right)^{1/2} e^{-x_0^2} \tag{B12}$$

$$I^{(1)} = \frac{p}{u\,m}\left(1 - \frac{p}{m\,n\,u^2}\right) \mathrm{erf}(x_0) + \frac{1}{2\sqrt{\pi}}\frac{n}{u^2}\left(\frac{2p}{m\,n}\right)^{3/2} e^{-x_0^2} \tag{B13}$$

$$I^{(2)} = \frac{3p}{u\,m}\left(1 + \frac{5}{3}\frac{p}{m\,n\,u^2}\right) \mathrm{erf}(x_0) + \frac{3}{2\sqrt{\pi}}\frac{n}{u^2}\left(\frac{2p}{m\,n}\right)^{3/2} e^{-x_0^2} \tag{B14}$$

The source functions appearing in eqautions (33) and (37) are

$$\frac{1}{3} m u^2 I^{(2)} = \frac{m\,n}{2\sqrt{\pi}} V_0^{3/2} e^{-x_0^2} + u\,p\left(1 + \frac{5}{6x_0^2}\right) \mathrm{erf}(x_0) \tag{B15}$$

$$W = m u^2 \left(I^{(1)} - \frac{1}{3} I^{(2)}\right) = -\frac{8}{6}\frac{u\,p}{x_0^2} \mathrm{erf}(x_0) \tag{B16}$$

Figure captions

Figure 1. Schematic representation of the implanted ion pickup geometry. This velocity space diagram is a projection to the ecliptic plane in the solar frame of reference (the V_x axis points towards the sun). V_{SW} and V_c represent the velocities of the solar wind flow and the comet, respectively. It can be seen that the initial velocity of a newly born cometary ion in the solar wind frame of reference is $V_I = V_c - V_{SW}$ (if one neglects the outflow velocity of neutral cometary particles). The dashed line indicates the direction of the interplanetary magnetic field (IMF). B is the IMF magnitude, $V_{I,\perp}$ denotes the velocity component perpendicular to the IMF direction, while $V_{I,\parallel}$ is the field aligned velocity. This field aligned motion of the pickup ring generates a broad spectrum of magnetohydrodynamic turbulence. As a result of the strong wave - particle interaction process the pitch angles of the pickup-ring particles quickly become randomized in the solar wind frame of reference and they become distributed on a shell having a radius of V_I around the local solar wind velocity.

Figure 2. Variation of the relative Fermi scattering mean free path, velocity diffusion coefficient and magnetic turbulence power level along the subsolar flow line. The dotted and dashed lines represent H^+ and O^+, respectively.

Figure 3. Variation of the neutral particle concentration, charge exchange scalelength and ionization lifetime along the subsolar flow line. The dotted and dashed lines represent H^+ and O^+, respectively.

Figure 4. Flow velocity deceleration along the subsolar flow line. The individual curves represent the contribution of the following processes: H^+ ion implantation, O^+ ion implantation, H^+ diffusion, O^+ diffusion, solar wind charge exchange loss, H^+ charge exchange loss, and O^+ charge exchange loss.

Figure 5. Variation of the flow velocity, Mach number, ion concentration and pressure along the subsolar flow line. The solid lines in the concentration and pressure diagrams represent the solar wind, while the dotted and dashed lines represent H^+ and O^+, respectively.

Figure 6. Implanted H^+ distribution functions along the subsolar flow line.

Figure 7. Implanted O^+ distribution functions along the subsolar flow line. The diamonds represent the phase space density values observed by VEGA-1 right before it crossed the bow shock.

Figure 8. Variation of the effective implanted heavy ion temperature (defined in the text) along the subsolar flow line.

Figure 9. Calculated implanted H^+ distribution functions along the VEGA-1 trajectory.

Figure 10. Calculated implanted O^+ distribution functions along the subsolar flow line. The diamonds represent the phase space density values observed by VEGA-1 right before it crossed the bow shock.

Figure 11. A comparison of the calculated and measured effective heavy ion temperature values along the VEGA-1 trajectory.

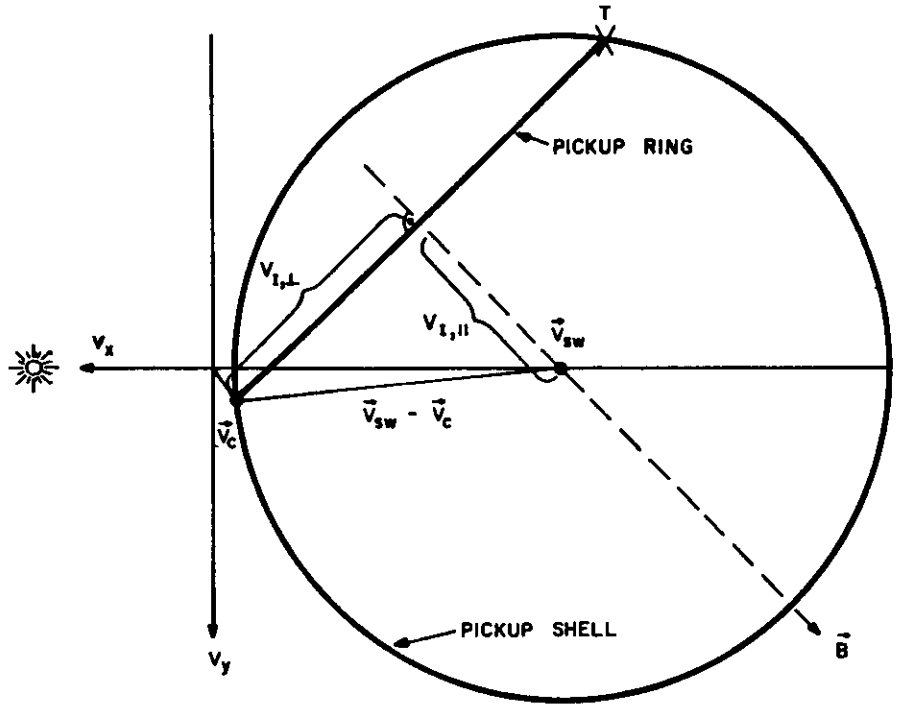

Figure 1.

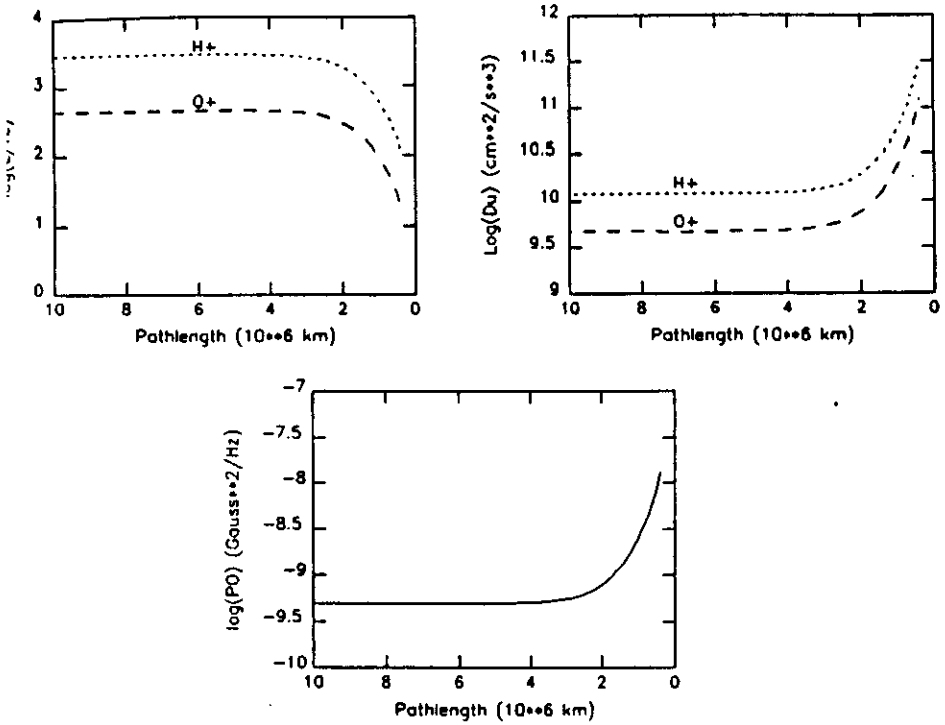

Figure 2.

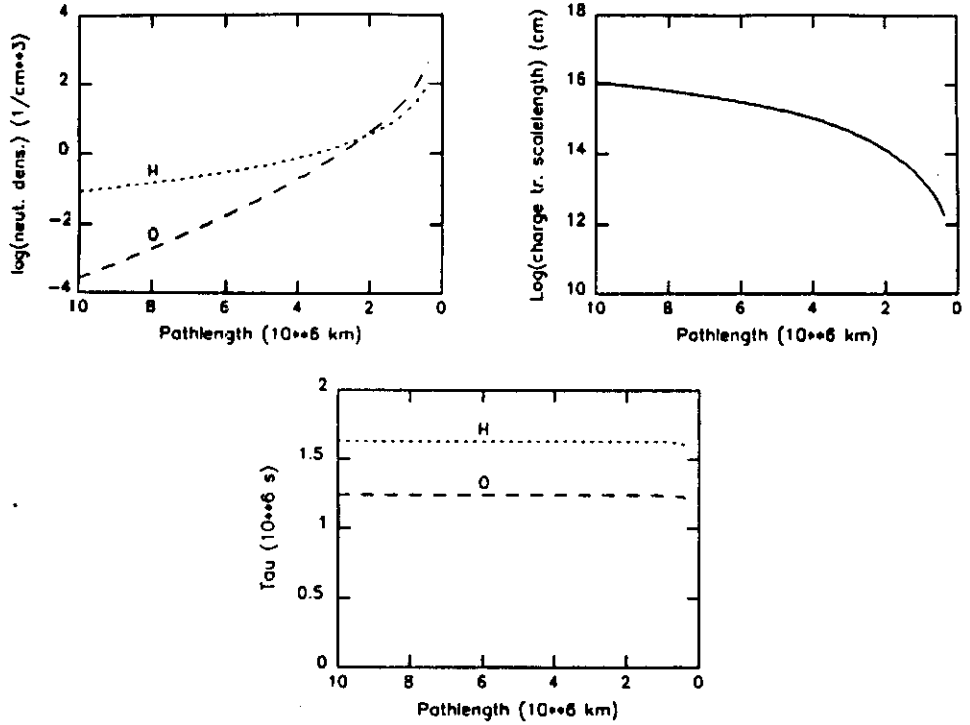

Figure 3.

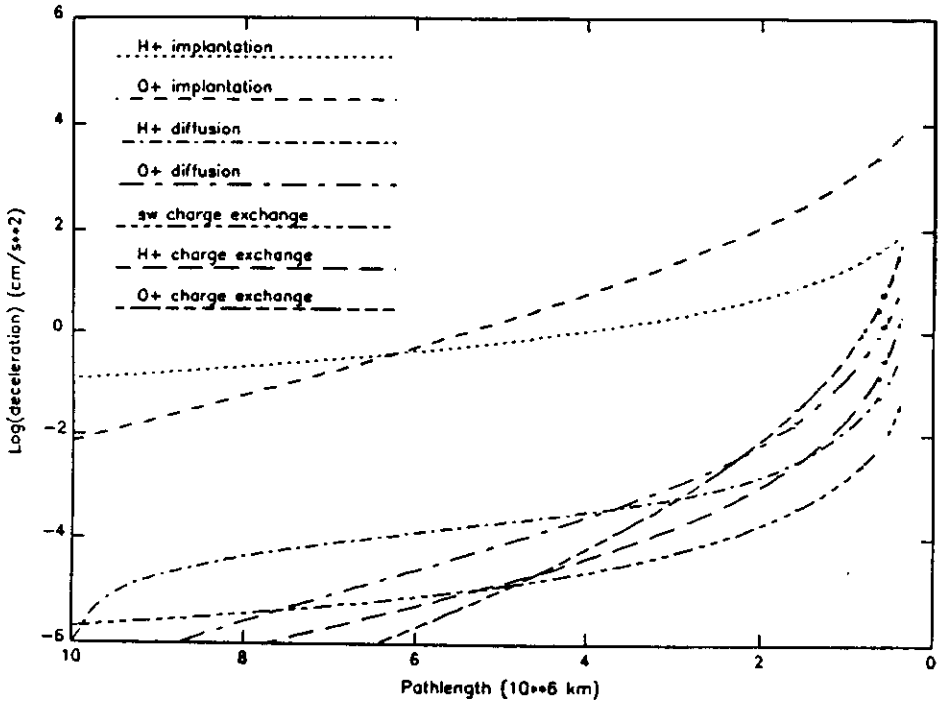

Figure 4.

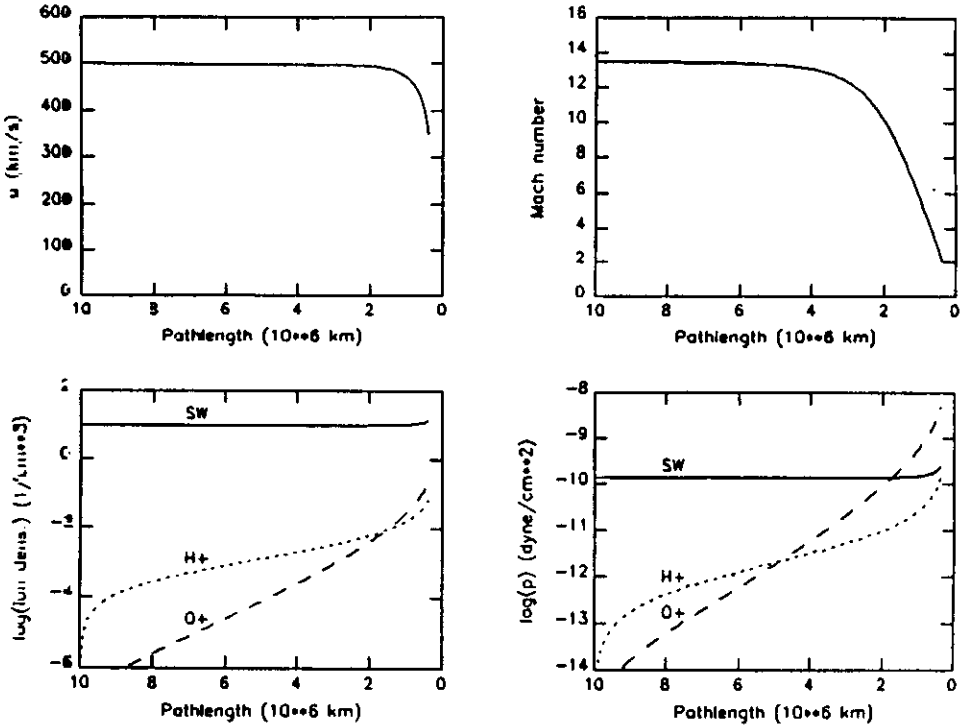

Figure 5.

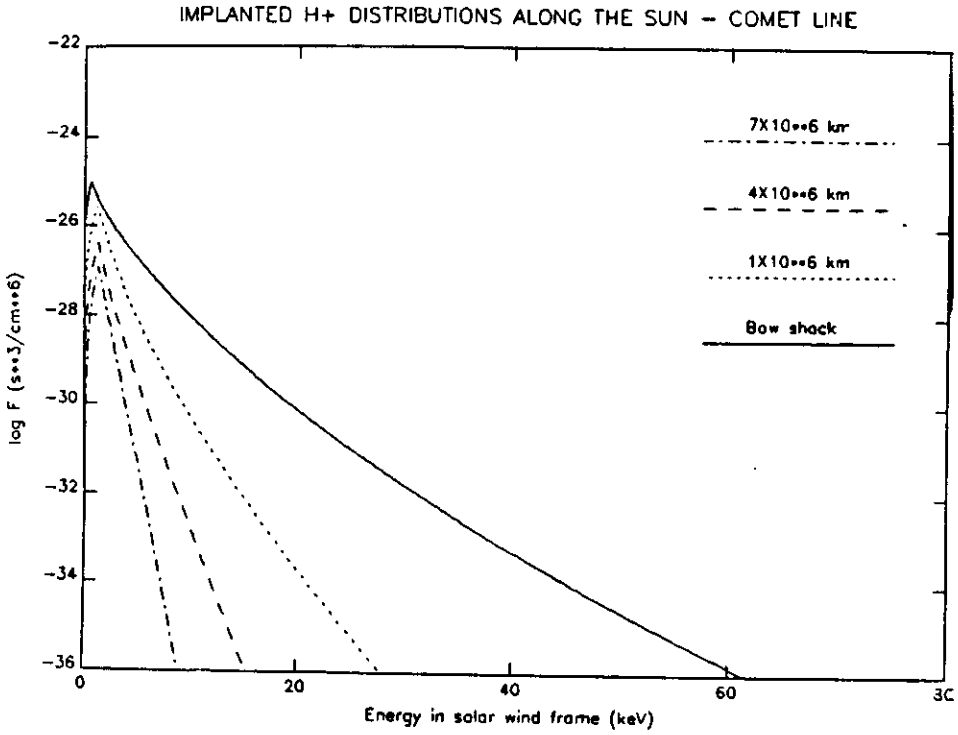

Figure 6.

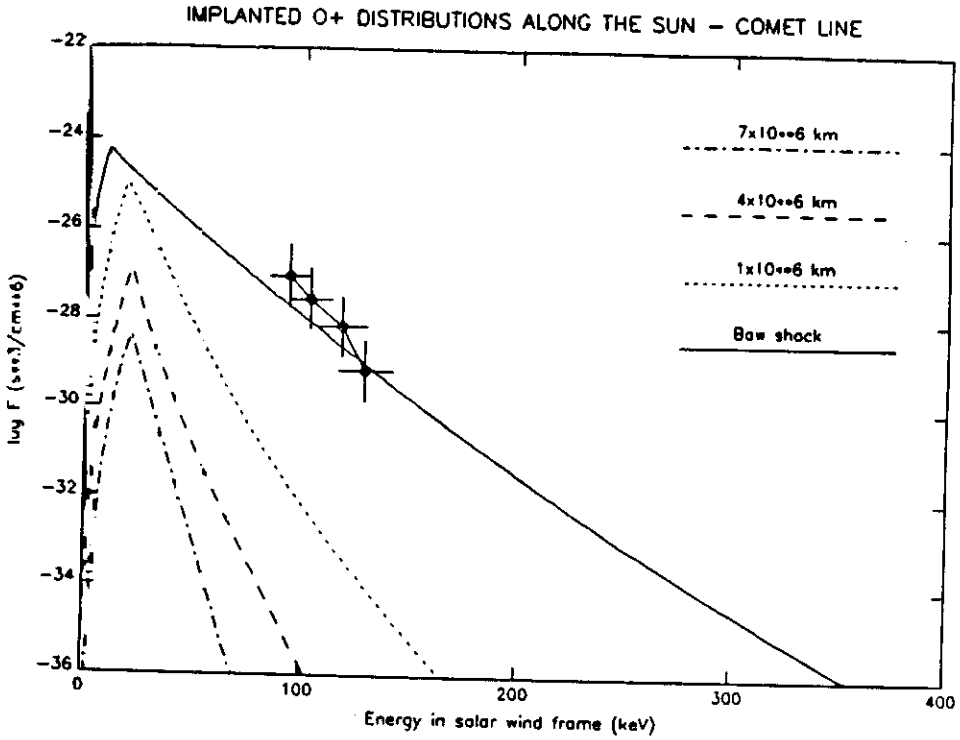

Figure 7.

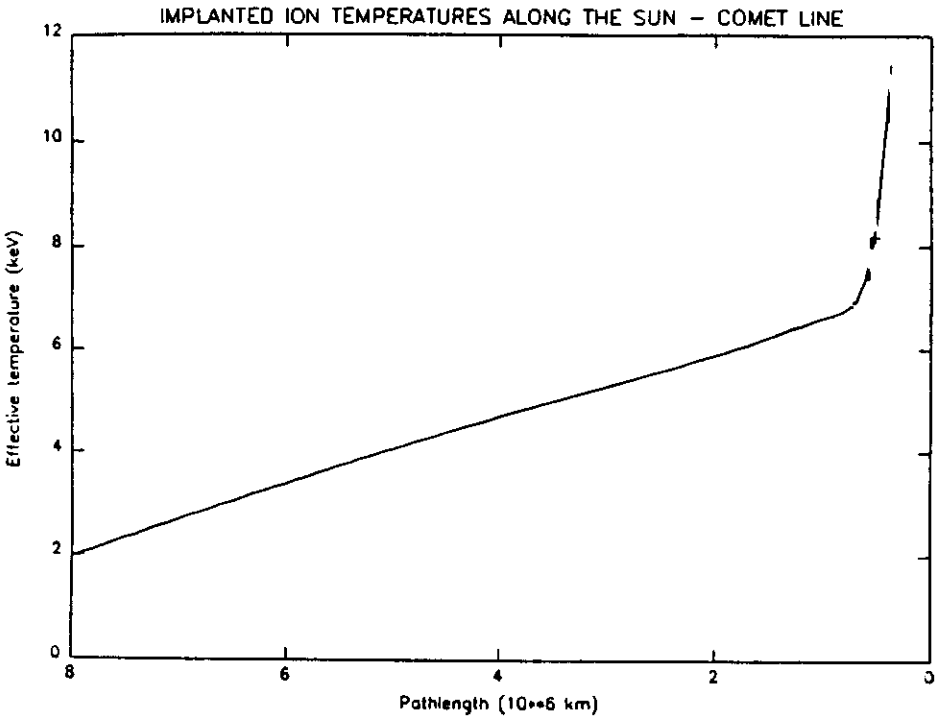

Figure 8.

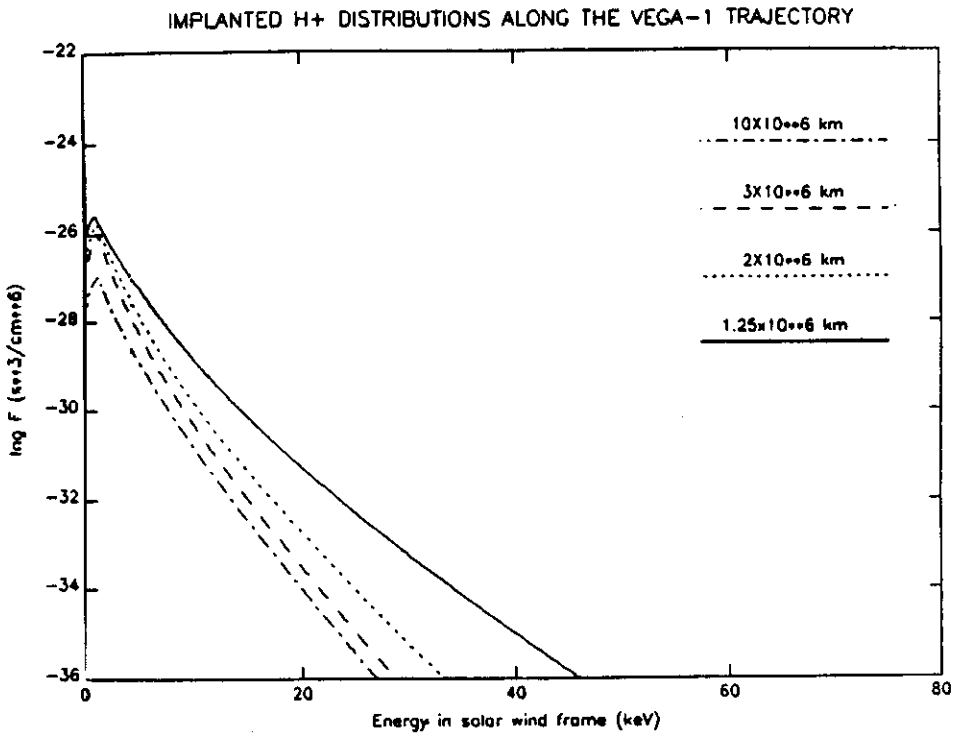

Figure 9.

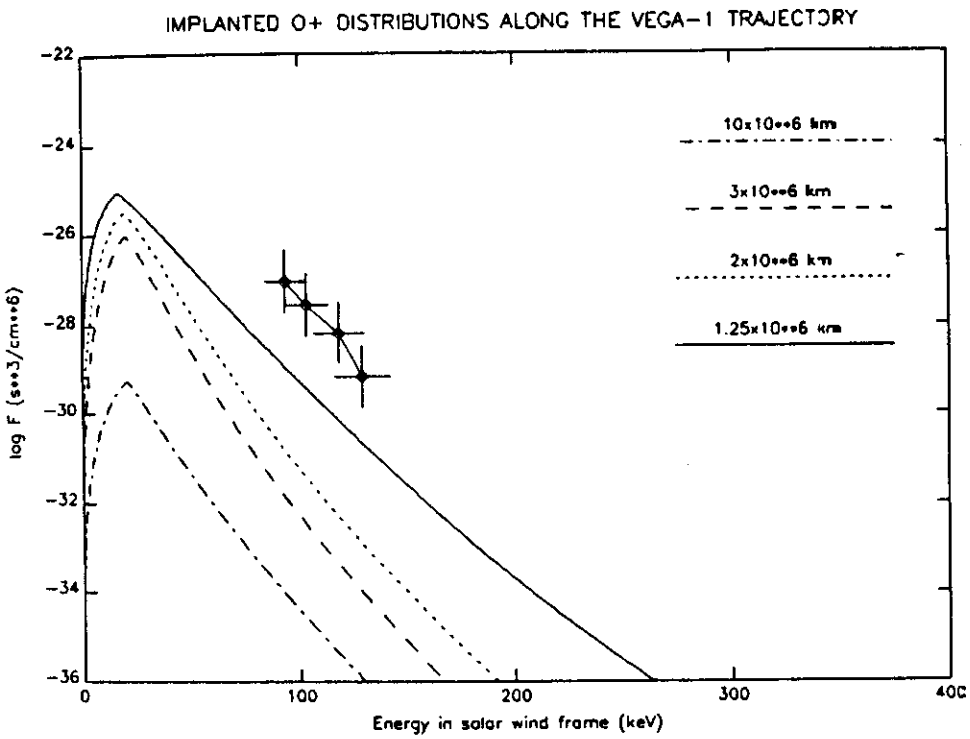

Figure 10.

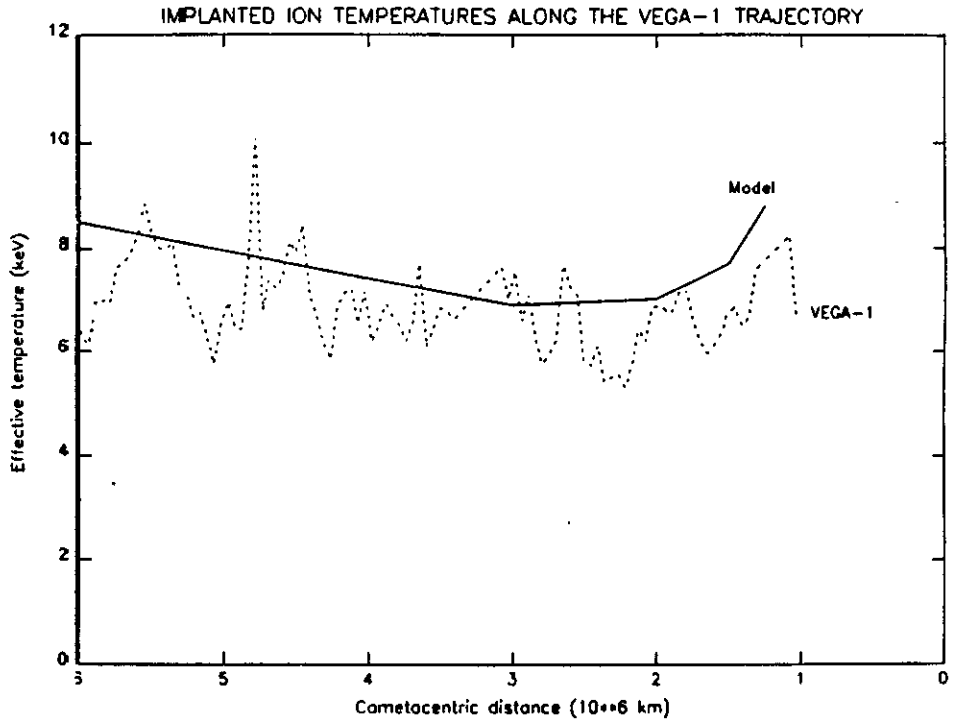

Figure 11.